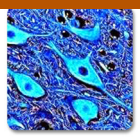

Journal of Histology & Histopathology
ISSN 2055-091X | Volume 4 | Article 14

HOAJ
Herbert Open Access Journals

Special Section | Morphological bases of human diseases | Methodology Open Access

Immunohistochemical identification of stent-based ablation lesions in the superior vena cava and pulmonary veins

Tim Vandecasteele[1*], Stijn Schauvliege[2], Tim Boussy[3], Matthew Philpott[4], Eli Clement[4], Lisse Vera[5], Pieter Cornillie[1], Ward De Spiegelaere[1], Glenn Van Langenhove[4], Gunther van Loon[5] and Wim Van den Broeck[1]

*Correspondence: Tim.Vandecasteele@Ugent.be

[1]Department of Morphology, Faculty of Veterinary Medicine, Ghent University, Belgium.
[2]Department of Surgery and Anesthesia of Domestic animals, Ghent University, Belgium.
[3]Department of cardiology AZ Groeninge Kortrijk/ AZM Middelares Ghent, Belgium.
[4]Fulgur Medical, Bergstraat 21, 9820 Merelbeke, Belgium.
[5]Department of Large Animal Internal Medicine, Faculty of Veterinary Medicine, Ghent University, Belgium.

Abstract

Background: Ablation procedures, in the context of atrial fibrillation treatment, induce lesions which are difficult to visualize in an acute phase. This study sought to develop an immunohistochemical technique to evaluate and visualize microscopically the applied acute ablation lesions, which may enable an objective assessment of the lesions as this is crucial to determine lesion transmurality.

Methods: In the present study, an ablation procedure was performed in vivo in six pigs at the level of the cranial vena cava and in-vitro at the level of the ostia of the pulmonary veins using the same custom-made stents and delivery system. The antibody myosin MYBPC3 was used to visualize indirectly the denaturation process induced by the heating procedure. Subsequently, the histological images were processed by using Fiji software to make standardized sections which are objectively comparable.

Results: In all samples, the ablation lesions were visualized immunohistochemically and clearly identified to enable lesion measurement. The absence of transmural lesions was noticed in the samples which were exposed to an insufficient or an extreme high energy level or in the case the myocardial layer was divided by an intermediate fat layer.

Conclusions: During postmortem histopathologic evaluation of ablated tissue, this technique offers a method to specifically determine the grade of muscle protein denaturation and to assess the degree of transmurality. Moreover, this study highlights the importance of myocardial tissue shielded by connective, fat and/or charred tissue, from the penetrating ablation heat in the context of recurrence or persistence of atrial fibrillation.

Keywords: Antibody, atrial fibrillation, animal model, ablation, histopathology

Introduction

In men, atrial fibrillation (AF) is the most important cardiac arrhythmia with an increasing prevalence due to an ageing population [1,2]. Besides a medical treatment of AF, ablation of myocardial sleeve tissue is increasingly used [3]. AF is mainly caused by the elicitation of ectopic pulses from myocardial sleeve tissue and their conductance towards the heart [4]. Ablation includes the interruption of the transfer of these pulses by using a heat or cold source. During an ablation procedure, lesions are applied to the myocardial tissue, especially at the level of the pulmonary veins wall or less commonly at the wall of the superior vena cava, coronary sinus or interatrial septum [5]. During evaluation of preclinical or clinical ablation trials, a distinct histological determination of the applied lesions, in an acute stage without the presence of repair connective tissue, remains difficult as regular histological staining of ablated tissue fails to distinguish clearly denatured cells from intact cells. Consequently, an immunohistochemical technique might be

doi: 10.7243/2055-091X-4-14

valuable to visualize and delineate precisely and objectively the ablated lesions and to evaluate the grade of lesion transmurality. Transmural lesions can be the cornerstone for a successful ablation procedure as the use of the appropriate energy level will define the result of creating the required local lesion [6].

However, during chronic follow-up studies based on biopsies or postmortem evaluation, ingrown connective tissue can be stained histologically to differentiate damaged from intact myocardial tissue. Different histological staining techniques for chronic lesions have been described, such as masson trichrome, hematoxylin and eosin, and elastic-van Gieson stains [6-9].

In this study, a technique is described to visualize and delineate immunohistochemically acute porcine ablation lesions at the level of the cranial vena cava (equivalent of the superior vena cava in humans) and at the level of the ostia of the pulmonary veins.

Methods

Stent delivery

Superior vena cava

Six 1.5 month old pigs (pigs 1-6, **Table 1**), weighing between 40 and 45 kg were used in the animal trials performed at the IMMR institute, Paris, France according to the Ethical Committee approval number "Fulgur Medical 16-22". Pigs were anesthetized using 6 mg/kg propofol and 2 % isoflurane. In each pig, one custom-made stent was placed inside the proximal part of the cranial vena cava. More specific, by using angiography the ablation ring of the stent was positioned to target myocardial tissue. Delivery of the stent through the right auricle was performed using a custom-made delivery catheter, followed by angiographic evaluation of the stent position.

Pulmonary veins

Fresh cardiopulmonary sets of nine pigs of 60 kg (pigs 7-12, **Table 1**) were used in the in-vitro trials performed at the Faculty of Veterinary Medicine, Ghent, Belgium. In each set, one custom-made stent was placed inside an ostium of the pulmonary veins and afterwards the stent and the surrounding tissue was excised from the cardiopulmonary set.

Ablation procedure

Superior vena cava

The stent was heated wirelessly by placing the pig in a coil to induce a magnetic field between the stent and the coil as described by Vandecasteele et al. (2016) [10]. Each pig was treated with a different combination of stent diameter, ablation time and power (**Table 1**).

Pulmonary veins

The sample was placed inside a closed water-perfused circuit and heated wirelessly, by placing a coil around the stent and the surrounding ostium, for different time periods, flow rate and with different power settings.

Histology

Superior vena cava

All pigs were euthanized directly after the ablation proce-

Table 1. Overview of the treatment strategies of the different pigs with indication of the ablation time (s), the applied power (W/mm² or mT, kHz), flowrate (l/min) and stent size (mm).

	First treatment (s -W/mm²)	Second treatment (s - W/mm²)	Third treatment (s - W/mm²)	Implant size (mm)	Remarks
Pig 1	150 - 0.190	280 - 0.210	150 - 0.225	21	No circumferential wall contact
Pig 2	210 - 0.195	150 - 0.210	--	21	No circumferential wall contact
Pig 3	220 - 0.220	150 - 0.254	--	24	--
Pig 4	60 - 0.282	--	--	30	--
Pig 5	60 - 0.195	--	--	30	--
Pig 6	210 - 0.207	60 - 0.254	--	24	--
	mT/kHz	**Duration (s)**	**Flowrate (l/min)**	**Implant size (mm)**	--
Pig 7	3.03/368	90	0	18	--
Pig 8	3/368	180	0	18	--
Pig 9	3/368	180	0	18	--
Pig 10	3/368	90	1.25	21	--
Pig 11	3/368	90	1.25	21	--
Pig 12	2.5/368	90	2	21	--
Pig 13	3/368	180	2	21	--
Pig 14	/	/	0	18	--
Pig 15	/	/	2	21	--

doi: 10.7243/2055-091X-4-14

dure. After removal of the heart-lung package, a part of the right auricle and the cranial vena cava, including the stent, were dissected. Hereafter, the stent was removed from the longitudinally opened blood vessel. The part of the vena cava demonstrating the burned marking of the stent was cut out and fixed in 4% formaldehyde solution for 24 hours. Subsequently, the samples were stored in alcohol 70%. Prior to the dehydration steps, the endothelial scar markings were stained with tissue ink (**Figure 1**). The dehydration procedure occurred according to standard laboratory procedures and, subsequently, the samples were embedded in paraffin using a Microm tissue processor STP 420D (Prosan, Merelbeke, Belgium) and Microm embedding station EC 350-1 (Prosan), respectively. Sections of 5 µm were cut longitudinally on a Microm H360 microtome (Prosan).

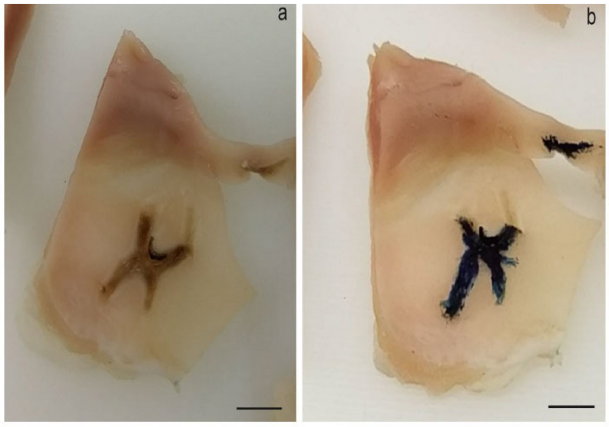

Figure 1. Ablated superior vena cava sample of pig 1 with an applied endothelial ablation lesion, before (**panel a**) and after applying the blue tissue ink (**panel b**), scalebar=0.5cm.

Pulmonary veins

The ablated tissue was removed from the stent and fixed, dehydrated, embedded and cut as described above.

Immunohistochemistry

The myocardial sleeve tissue of the cranial vena cava and the pulmonary veins of the different pigs was stained immunohistochemically with the polyclonal myosin marker MYBPC3 (K-16: sc-50115; Santa Cruz Biotechnology, Santa Cruz, CA, USA) to detect myosin-binding protein C (cardiac type), which is reactive with pig tissue and present in the myofibrils of cardiac and striated muscle tissue [**11**]. Immunostaining was performed using the Dako automated Autostainer Plus. No antigen retrieval was needed. Firstly, the sections were incubated for 5 min with 3% hydrogen peroxide and 30 min with rabbit serum. After primary antibody incubation for 60 min, secondary antibody (rabbit/anti-goat, biotinylated, polyclonal, 1:500; Dako, Glostrup, Denmark) was used for 30 min followed by streptavidin and horseradish peroxidase (streptavidin-HRP, 1:1500, Dako) for 30 min. Visualization was performed with DAB (Dako) for 5 min. The immunohistochemical sections were observed under the light microscope (Olympus BX61, Olympus DP73 camera, Olympus, Belgium).

Indirect lesion identification is done as follows. The antibody MYBPC3 positive regions (dark staining) will refer to intact myocardial tissue whereas the ablated parts (lighter staining) will be negative for the immunohistochemical staining.

Software processing

Free software Fiji was used to process and to standardize the images of the immunohistochemical sections by using the same threshold for each section (**Figure 2**) [**12**]. After color deconvolution (for haematoxylin and DAB) and duplicating the image, the threshold was set at zero and 90. Afterwards, the adapted image was overlaid with the original image at 50% opacity and flattened together. The scale bar was set and the images were measured.

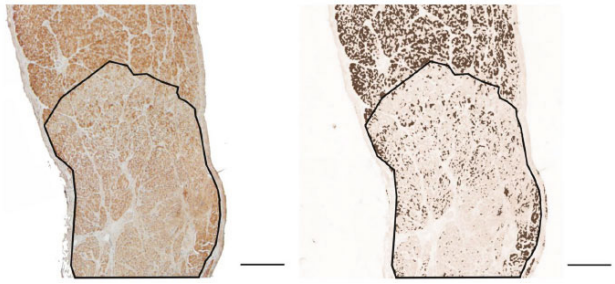

Figure 2. Immunohistological image of an ablated superior vena cava of pig 1 with a transmural lesion before (left) and after (right) Fiji software processing. The ablation lesion is contoured in both images, scale bar=250µm.

Results

The Fiji processed images showed the lesions more clearly compared to the original images as demonstrated in **Figure 2**. A gradual change of brown shades was observed, depending on the position of the observed spot. If this spot is located close to the position of the applied heat source, a lighter zone is noticed compared to a spot located further away from the heat source (**Figure 3**).

All immunohistochemical samples of the different pigs demonstrated clear ablation lesions, except of the two control samples (pigs 14 and 15, **Table 1**), which are visible on the sections as lighter zones compared to the non-ablated regions. These lighter zones also correspond with the tissue ink present at the endothelial side of the ablated region of the caudal vena cava sections. Some samples displayed transmural lesions (pigs 1, 2, 3, 4, 6, 8 and 13; **Figures 2-4** and **6**) whereas other samples demonstrated no transmural lesions with lighter stained myosin-denaturation-patterns

doi: 10.7243/2055-091X-4-14

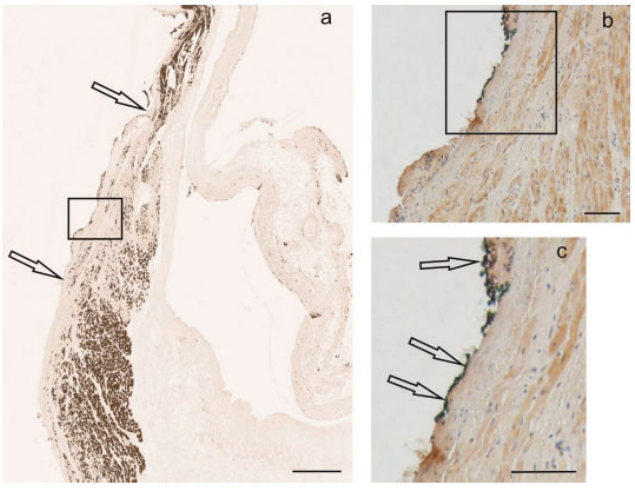

Figure 3. **Panel a:** Fiji-software-processed immuohistological image of an ablated superior vena cava of pig 6 with tissue ink applied (insert) at the endothelial side at the level of the heating spot (between two arrows), with the latter identifiable as the myosin proteins are almost all denatured at this level, scalebar=500µm. **Panel b**: Detail of panel a with the insert indicating the applied ink, scalebar=100µm. **Panel c**: Higher magnification of the insert indicated in panel b with the arrows indicating the applied blue tissue ink, scale bar=100µm.

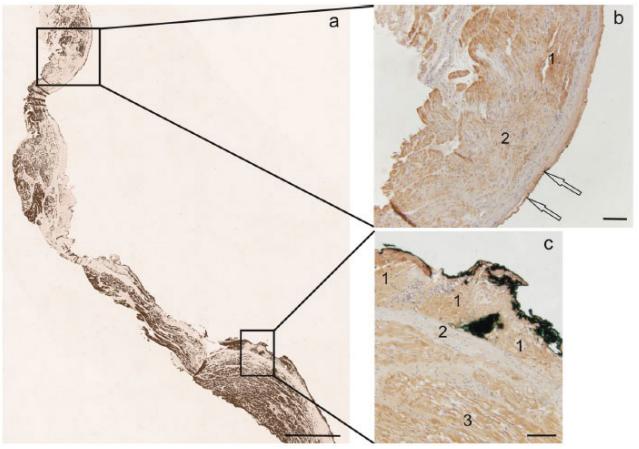

Figure 4. **Panel a**: Fiji-software-processed immunohistological image of an ablated superior vena cava of pig 4 with tissue ink applied at the endothelial side at the level of the heating spot, indicated by the arrows in panel b, scale bar of panel a=1mm. **Panel b**: Higher magnification of the delimited area in panel a, indicating both a non-ablated region (1) and ablated region (2), scale bar=100µm. **Panel c**: Highly enlarged detail of panel a, demonstrating an insulating barrier consisting of charred (1) and connective tissue (2) between the heating area (indicated by the blue ink) and the intact myocardial tissue (3), scale bar=100µm.

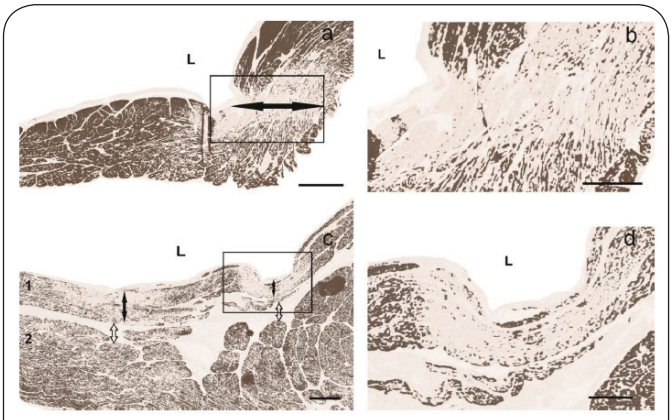

Figure 5. Both images (a and c) are derived from ablation trials with the same setting and conditions. **Panel a**: Fiji-software-processed immunohistological image of an ablated pulmonary vein of pig 10. The arrow indicates an ablation lesion of approximately 2.38 mm, L =lumen, scalebar=1mm. **Panel b**: detail of panel a, indicated by the box, in which the loss of staining is visualized, L=lumen, scalebar= 0.5mm.
Panel c: Fiji-software-processed immunohistological image of an ablated pulmonary vein of pig 11. The black arrows indicate two ablation spots (0.6mm and 1mm) in myocardial layer 1. The white arrows indicate the fat layer between myocardial layer 1 and 2, L=lumen, scalebar=1mm. **Panel d**: detail of panel c, indicated by the box, in which the lighter staining visualizes the transition of normal tissue to ablated tissue, L=lumen, scalebar=0.5mm.

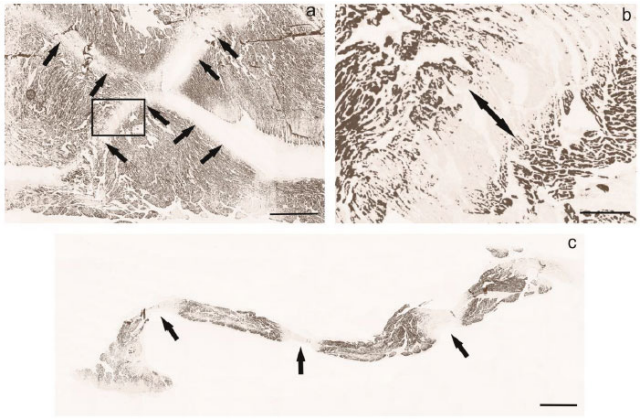

Figure 6. **Panel a**: Fiji-software-processed immunohistological image of an ablated pulmonary vein of pig 12. The section was cut parallel to and 10µm from the endothelium. The arrows indicate the diamond-shaped ablation lesion which matches perfectly the organization of the struts, scale bar=2mm.
Panel b: detail of panel a, indicated by the box, in which the loss of staining is indicated in higher magnification by the double arrow, scale bar=0.4mm. **Panel c**: Fiji-software-processed immunohistological image of an ablated pulmonary vein of pig 13. The section was cut longitudinally and the arrows indicate several transmural ablation lesions at regular distances, due to the structure of the stent. Scale bar=2mm.

at different depths, measured from the endothelium at the level of the applied ink. All samples included, the ablation depth ranged from 0.45mm to 2.38mm.

If superficially induced charring and/or physiologic connective tissue was present between themyocardial tissue and the

doi: 10.7243/2055-091X-4-14

heat source, little or no myosin denaturation was observed (**Figure 4**). Often, pulmonary vein samples demonstrated several layers of myocardial tissue separated from each other by fat and connective tissue. In that case, no myosin denaturation was noticed in the myocardial sleeve layer located at the adventitial side of the fat whereas at the same level, a transmural lesion could be observed in the myocardial tissue located at the endothelial side.

Two samples of pulmonary vein tissue were ablated under the same conditions and with the same power setting. The sample in which no fat was present demonstrated an ablation lesion, more than twice the depth compared to the lesion observed in the sample in which the myocardial sleeve layer was divided in two by an intermediate layer of fat (**Figure 5**).

Several immunohistochemical sections of the pulmonary veins provided an ablation pattern which is in accordance with the structure of the stent. The stent is build-up by a number of struts and the diamond-like shape of the struts was recognized in the ablated tissue (**Figure 6**).

Discussion

The standard histological staining methods fail to make a clear distinction between destructed tissue and intact tissue. Moreover, with these techniques it is sometimes hard to visualize objectively the gradual reduction of heat intensity when sampling away from the ablation point. A misinterpretation of the grade of heat penetration, based on a regular histological staining, could be caused by an unequal fixation of the tissue, due to a variable tissue thickness as no control is available. Further, regular histological staining methods are not directly linked with the process occurring in ablated, destructed or denatured tissue but offer an overview of the present tissue types without discriminating between heated and non-heated tissue. The supra-vital staining with tetrazolium is frequently used to distinguish non-vital from vital tissue [**13**]. However, in the case of determining the grade of transmurality, more detail or histological images on higher magnification are required which is not possible with this supra-vital staining. On the other hand, immunohistochemical staining with antibody myosin MYBPC3 visualizes exactly the gradual denaturation of the muscle protein myosin, which is, according to Tornberg (2005) [**14**], the first characteristic of muscle tissue that will be affected during a heating process.

The evaluation of the degree of chronic ablation lesions will offer less difficulties as ingrown connective tissue will replace destructed cardiac tissue. However, in chronic samples, the described immunohistochemical technique will also be valuable as it detects viable myocardial tissue.

The use of a too high or too low temperature during an ablation procedure will fail to achieve a transmural lesion. The application of extreme temperatures or distribution of energy on a small area will lead to superficial endothelial charring, which reduces energy transfer to the underlying cardiac muscle. On the other hand, myocardial sleeve tissue fans out distally, thus heart muscle fibers, covered by fat and connective tissue, could get shielded from the ablating heat source. Some samples, investigated in this study, demonstrated that heat penetration into the venous wall was limited due to the insulating effect of connective, fat and/or charred tissue.

This could be a reason why recurrence of ectopic electrical conductance is frequently seen after ablation procedures. The constitution of the venous wall needs to be considered in case of ablation failure, AF recurrence is noticed or electrical conductance persists.

Conclusions

This study demonstrates an immunohistochemical staining technique with the MYBPC3 antibody to visualize and to asses objectively acute ablation lesions. Moreover, the importance of the insulating role on heat transfer of endothelial charring, fat or connective tissue is emphasized.

Competing interests

The authors declare that they have no competing interests.

Authors' contributions

Authors' contributions	TV	SS	TB	MP	EC	LV	PC	WDS	GVL	GL	WVB
Research concept and design	✓	✓	✓	--	--	--	--	--	--	✓	✓
Collection and/or assembly of data	✓	✓	✓	✓	✓	✓	--	--	--	--	--
Data analysis and interpretation	✓	--	--	✓	✓	--	✓	✓	--	✓	--
Writing the article	✓	✓	--	--	--	✓	--	--	✓	--	✓
Critical revision of the article	--	--	--	--	--	--	✓	✓	✓	✓	✓
Final approval of article	✓	✓	✓	✓	✓	✓	✓	✓	✓	✓	✓
Statistical analysis	--	--	--	--	--	--	--	--	--	--	--

Acknowledgements

The authors thank Lobke De Bels for the technical assistance.

Publication history

EIC: Gaetano Giuseppe Magro, University of Catania, Italy.
Received: 04-Oct-2017 Final Revised: 07-Nov-2017
Accepted: 13-Nov-2017 Published: 24-Nov-2017

References

1. Roberts SA, Diaz C, Nolan PE, Salerno DM, Stapczynski JS, Zbrozek AS, Ritz EG, Bauman JL and Vlasses PH. **Effectiveness and costs of digoxin treatment for atrial fibrillation and flutter**. *Am J Cardiol*. 1993; **72**:567-73. | Article | PubMed
2. Iwasaki YK, Nishida K, Kato T and Nattel S. **Atrial fibrillation pathophysiology: implications for management**. *Circulation*. 2011; **124**:2264-74. | Article | PubMed
3. Calkins H, Kuck KH, Cappato R, Brugada J, Camm AJ, Chen SA, Crijns HJ, Damiano RJ, Jr., Davies DW and DiMarco J et al. **2012 HRS/EHRA/ECAS expert consensus statement on catheter and surgical ablation of atrial fibrillation: recommendations for patient selection, procedural techniques, patient management and follow-up, definitions, endpoints, and research trial design**. *J Interv Card Electrophysiol*. 2012; **33**:171-257. | Article | PubMed
4. Haissaguerre M, Jais P, Shah DC, Takahashi A, Hocini M, Quiniou G, Garrigue S, Le Mouroux A, Le Metayer P and Clementy J. **Spontaneous initiation of atrial fibrillation by ectopic beats originating in the pulmonary veins**. *N Engl J Med*. 1998; **339**:659-66. | Article | PubMed
5. Oral H, Knight BP, Tada H, Ozaydin M, Chugh A, Hassan S, Scharf C, Lai SW, Greenstein R, Pelosi F, Jr., Strickberger SA and Morady F. **Pulmonary vein isolation for paroxysmal and persistent atrial fibrillation**. *Circulation*. 2002; **105**:1077-81. | Article | PubMed
6. Kowalski M, Grimes MM, Perez FJ, Kenigsberg DN, Koneru J, Kasirajan V, Wood MA and Ellenbogen KA. **Histopathologic characterization of chronic radiofrequency ablation lesions for pulmonary vein isolation**. *J Am Coll Cardiol*. 2012; **59**:930-8. | Article | PubMed
7. Accord RE, van Suylen RJ, van Brakel TJ and Maessen JG. **Post-mortem histologic evaluation of microwave lesions after epicardial pulmonary vein isolation for atrial fibrillation**. *Ann Thorac Surg*. 2005; **80**:881-7. | Article | PubMed
8. Deneke T, Khargi K, Muller KM, Lemke B, Mugge A, Laczkovics A, Becker AE and Grewe PH. **Histopathology of intraoperatively induced linear radiofrequency ablation lesions in patients with chronic atrial fibrillation**. *Eur Heart J*. 2005; **26**:1797-803. | Article | PubMed
9. Ranjan R, Kato R, Zviman MM, Dickfeld TM, Roguin A, Berger RD, Tomaselli GF and Halperin HR. **Gaps in the ablation line as a potential cause of recovery from electrical isolation and their visualization using MRI**. *Circ Arrhythm Electrophysiol*. 2011; **4**:279-86. | Article | PubMed Abstract | PubMed FullText
10. Vandecasteele T, Boussy T, Philpott M, Clement E, Schauvliege S, W VDB, G VANL, Cornillie P and G VANL. **A Preclinical Study of an Implanted Device in the Pulmonary Veins, Intended for the Treatment of Atrial Fibrillation in an Ovine Model**. *Pacing Clin Electrophysiol*. 2016; **39**:822-9. | Article | PubMed
11. Winegrad S. **Cardiac myosin binding protein C**. *Circ Res*. 1999; **84**:1117-26. | Article | PubMed
12. Schindelin J, Arganda-Carreras I, Frise E, Kaynig V, Longair M, Pietzsch T, Preibisch S, Rueden C, Saalfeld S, Schmid B, Tinevez JY, White DJ, Hartenstein V, Eliceiri K, Tomancak P and Cardona A. **Fiji: an open-source platform for biological-image analysis**. *Nat Methods*. 2012; **9**:676-82. | Article | PubMed Abstract | PubMed FullText
13. Calcutt G. **Supra-vital staining of striated muscle with tetrazolium compounds**. *Nature*. 1952; **170**:42. | PubMed
14. Tornberg E. **Effects of heat on meat proteins - Implications on structure and quality of meat products**. *Meat Sci*. 2005; **70**:493-508. | Article | PubMed

Citation:
Vandecasteele T, Schauvliege S, Boussy T, Philpott M, Clement E, Vera L, Cornillie P, De Spiegelaere W, Van Langenhove G, van Loon G and Van den Broeck W. **Immunohistochemical identification of stent-based ablation lesions in the superior vena cava and pulmonary veins**. *J Histol Histopathol*. 2017; **4**:14.
http://dx.doi.org/10.7243/2055-091X-4-14